

INFLUENCE OF ANGLE OF ATTACK ON SYNTHETIC JET EFFECTIVENESS AS FOUND WITH COEFFICIENT OF MOMENTUM

Mark A. Feero

Institute for Aerospace Studies
University of Toronto
4925 Dufferin Street, Toronto, ON, Canada
M3H 5T6
m.feero@mail.utoronto.ca

Sebastian D. Goodfellow

Department of Mechanical and Industrial Engineering
University of Toronto
5 King's College Road, Toronto, ON, Canada
M5S 3G8
sebi.goodfellow@utoronto.ca

Philippe Lavoie

Institute for Aerospace Studies
University of Toronto
4925 Dufferin Street, Toronto, ON, Canada
M3H 5T6
lavoie@utias.utoronto.ca

Pierre E. Sullivan

Department of Mechanical and Industrial Engineering
University of Toronto
5 King's College Road, Toronto, ON, Canada
M5S 3G8
sullivan@mie.utoronto.ca

ABSTRACT

The influence of periodic excitation from a synthetic jet actuator on the flow separation over a NACA 0025 airfoil at an angle of attack of 10° was investigated. Experiments were performed in a low-speed wind tunnel at a chord-based Reynolds number $Re_c = 10^5$. At $Re_c = 10^5$, the boundary layer separates and fails to reattach at angles of attack from $0 - 10^\circ$. When the boundary layer was forced at a momentum coefficient $C_\mu = 2.47 \times 10^{-2}$ and excitation frequency $f_e = 970$ Hz, the vortex shedding associated with the uncontrolled case was eliminated and the drag coefficient was reduced by 22%. These results were compared to previous work at $\alpha = 5^\circ$ on the same airfoil by Goodfellow *et al.* (2012), who found that a drag reduction of 52% was achieved at $C_\mu = 3.09 \times 10^{-3}$. The results suggest that as the angle of attack is increased from 5° to 10° , the synthetic jet actuator must transfer more momentum to the separated boundary layer in order to cause drag reduction.

INTRODUCTION

The operation of airfoils at low Reynolds number is of interest in a number of applications including low-speed unmanned aerial vehicles (UAVs), wind turbines, and low-speed/high-altitude aircraft. Standard airfoil profiles are designed for optimal aerodynamic performance at high Reynolds number where inertial effects dominate the flow. At chord-based Reynolds numbers less than 10^6 , significant performance deterioration is experienced (Lissaman, 1983). Flow separation on airfoils is particularly prevalent at low Reynolds number due to the interaction of the laminar boundary layer on the suction surface with an adverse pressure gradient. Even at low angles of attack, the adverse pressure gradient may be strong enough to cause the flow to separate (e.g. Yarusevych *et al.* (2006)).

The use of periodic excitation applied locally at the surface has shown promise as a means of separation control on

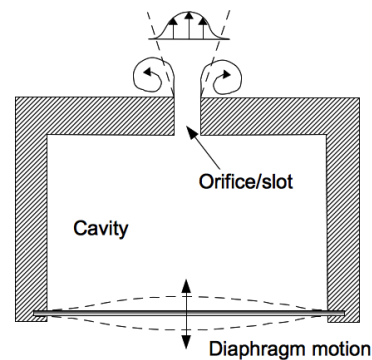


Figure 1: Synthetic jet actuator schematic.

low Reynolds number airfoils (e.g. Amitay *et al.* (2001); Tian *et al.* (2007)). Active control devices using periodic excitation interacts with the instabilities associated with the separated shear layer. A common zero-net-mass-flux fluidic actuator is the synthetic jet (Figure 1). A synthetic jet actuator (SJA) is composed of a vibrating diaphragm mounted in a cavity with an orifice/slot leading to the surface where control is desired. Deformation of the diaphragm causes the working fluid to be alternately expelled and ingested by the cavity, thereby adding momentum (but not mass) to the flow (Smith & Glezer, 1998). The net momentum transferred to the flow by the SJA is due to the formation of a vortex pair at the orifice/slot edge(s) during the expulsion phase. As the vortices detach and move away from the orifice, the resulting velocity profile resembles that of a 2D jet.

An extensive review by Greenblatt & Wygnanski (2000) found that the majority of investigations using periodic excitation on airfoils described an optimum dimensionless frequency within the range $0.1 \leq F^+ \leq 4$, where $F^+ = f_e X_{te} / U_\infty$, f_e is excitation frequency, U_∞ is freestream velocity and X_{te} is the streamwise distance from the actua-

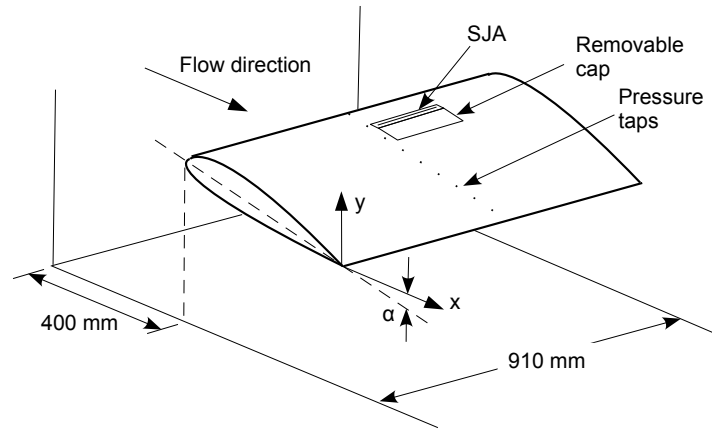


Figure 2: Schematic of the experimental setup in the wind tunnel.

tor to the trailing edge. However, some studies (Amitay *et al.*, 2001; Tian *et al.*, 2007; Goodfellow *et al.*, 2012) using synthetic jet actuation have found that optimal aerodynamic performance was achieved at excitation frequencies $F^+ > 10$. The reason for this wide range of effective frequencies may be due to the fact that there are multiple characteristic frequencies associated with flow separation. Tian *et al.* (2007) showed that two nonlinearly-coupled dominant frequencies are present in fully-separated flow: the wake frequency, f_{wake} , and the shear layer frequency, f_{SL} .

The effect of excitation amplitude for synthetic jet actuators is characterized using the momentum coefficient C_μ , defined as,

$$C_\mu = \frac{\bar{I}_j}{1/2\rho U_\infty^2 c}, \quad (1)$$

where ρ is the fluid density, c is chord length and \bar{I}_j is the time-averaged jet momentum per unit length during expulsion, given by,

$$\bar{I}_j = \rho d \frac{1}{T/2} \int_0^{T/2} U_j^2(t) dt, \quad (2)$$

where d is the slot width, T is the period of oscillation and U_j is the jet velocity at the exit plane.

Amitay *et al.* (2001) investigated the influence of C_μ on separation control of a circular-leading-edge NACA airfoil operating between $3.1 \times 10^5 < Re_c < 7.25 \times 10^5$ using a pair of synthetic jet actuators. The authors found that a certain value of C_μ (on the order $C_\mu \sim 10^{-3}$) was required to cause the flow to reattach, and this value decreased as the actuators were positioned closer to the separation point. Tian *et al.* (2007) used both amplitude-modulated (AM) and burst-modulated (BM) synthetic jet actuation to optimize the lift-to-drag ratio on a post-stalled NACA 0025 airfoil at $Re_c = 10^5$ and $\alpha = 20^\circ$. A closed-loop control strategy was able to fully reattach the flow and increase lift-to-drag by a factor of 2 for $C_\mu \sim 10^{-4} - 10^{-5}$. BM forcing was used to target both f_{wake} and f_{SL} while using considerably less power than standard periodic excitation. Goodfellow *et al.* (2012) used synthetic jet actuation to control separation on

a NACA 0025 airfoil operating at $Re_c = 10^5$ and an angle of attack $\alpha = 5^\circ$. A 50% reduction in drag was observed when the momentum coefficient reached a threshold value of $C_\mu \sim 10^{-3}$ (on the same order as Amitay *et al.* (2001)). Below the threshold value, negligible gain in aerodynamic performance was achieved. No further reduction in drag was seen beyond the threshold value of C_μ .

This paper discusses the impact of a synthetic jet actuator on the separated flow over a NACA 0025 airfoil at $\alpha = 10^\circ$ and compares the results to previous studies at $\alpha = 5^\circ$ by Goodfellow *et al.* (2012). All experiments are performed at a chord-based Reynolds number $Re_c = 10^5$. The goal is to use synthetic jet actuation to promote flow reattachment, thereby improving aerodynamic performance. In particular, the drag coefficient is sought to be reduced. The influence of the SJA momentum coefficient on drag reduction at constant excitation frequency is examined.

EXPERIMENTAL APPARATUS AND METHOD

The experiments were conducted in a low-turbulence horizontal recirculating wind tunnel located in the Department of Mechanical and Industrial Engineering at the University of Toronto. The 5 m long test section is 0.91 m wide and 1.22 m tall. The NACA 0025 airfoil has a chord length $c = 300$ mm and spans the width of the test section 400 mm downstream of the contraction (Figure 2). The model has 65 static pressure taps installed along the chord at midspan, with an equal amount of taps on the top and bottom surfaces. The tunnel is operated at a freestream velocity of approximately $U_\infty = 5$ m/s such that the chord-based Reynolds number is $Re_c = 10^5$. The freestream velocity is monitored using a pitot tube connected to a 0.5 inH2O pressure transducer, with an uncertainty of $\sim 2.5\%$ at $U_\infty = 5$ m/s. The angle of attack of the model is set using a digital protractor with an uncertainty of $\pm 0.05^\circ$.

The SJA is driven by four axisymmetric Thunder TH-5C piezoelectric actuators produced by Face International Corporation. The TH-5C reaches its maximum deflection of 0.173 mm when an AC voltage of 420 V_{p-p} (peak-to-peak) is applied. Oscillation of the piezoelectric actuators inside the cavity causes the working fluid to be alternately expelled and ingested through at 140×0.5 mm slot. The actuators are mounted on the side wall of the cavity such that their motion is perpendicular to the motion of the fluid through the slot, as shown in Figure 3. The input signal

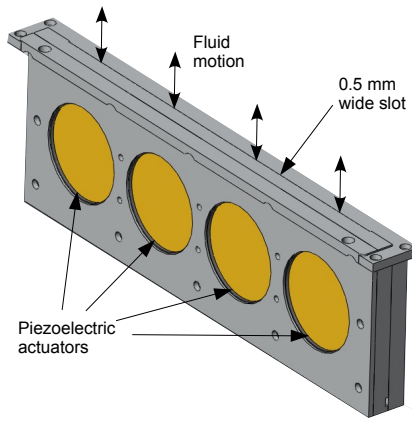


Figure 3: Synthetic jet actuator driven by four piezoelectric actuators.

that drives the actuators is created by a GW Instek GFG-8216A function generator and amplified by a high-voltage amplifier with a gain of 100 and a maximum output voltage of 400 V_{p-p} .

Synthetic jet forcing is applied over $\sim 15\%$ of the airfoil span. A 160 mm wide slot cut out of the airfoil model allows the streamwise location of the jet orifice to be varied from 58 mm to 101 mm from the leading edge. The SJA was secured in a fixed position with four screws and the remainder of the slot was covered by a removable cap machined to match the airfoil curvature (Figure 2). At an angle of attack of 10° , the flow separates 54 mm downstream of the leading edge (Yarusevych *et al.*, 2006). Therefore, at its most upstream position the jet is approximately 4 mm downstream of the separation point. Due to physical constraints, the jet could not be placed upstream of separation at $\alpha = 10^\circ$.

Flow velocity was measured using hot-wire anemometry. A Dantec 56C01 main unit with a 56C17 constant temperature anemometry bridge was used to measure the voltage from a single hot-wire probe. The anemometer signal was acquired using a National Instruments 4472 24-bit digital acquisition board connected to a desktop computer with LabView software. The hot-wire probe was calibrated before and after each experiment using a Dantex 55D90 calibration unit. The calibration data was fit according to King's Law.

Prior to performing flow control experiments, the SJA was characterized in quiescent conditions by measuring the frequency response of the exit-plane jet velocity for a range of input amplitudes. The SJA was clamped in a rigid stand and a hot-wire probe was positioned several millimetres inside the slot such that the ingestion phase was also captured. At each amplitude and forcing frequency, $N = 10^5$ data points were acquired at a sampling rate $f_s = 20 \text{ kHz}$. The hot-wire and function generator signals were sampled simultaneously. Since the jet velocity is a periodic quantity, a standard time-mean does not provide useful information and instead the phase-averaged jet velocity was computed as suggested by Reynolds & Hussain (1972). Phase-averaged velocity profiles were computed by dividing the total data set into blocks that each represent a particular phase location and contain $n = 500$ points. The resolution in phase was $\Delta\theta = 1.8^\circ$.

The drag coefficient will be used as a means of measuring the aerodynamic performance of the airfoil. At low Reynolds number, the airfoil drag can be estimated using a

control volume analysis (Van Dam, 1999) as,

$$C_D = \frac{2}{U_o^2 c} \int_{y_1}^{y_2} (U_o^2 - U^2) dy, \quad (3)$$

where y_2 and y_1 are the upper and lower wake boundaries, respectively, U is the mean streamwise velocity and U_o is the outer flow velocity at the measurement plane. In recent work by Neatby & Yarusevych (2012), the authors demonstrated that estimating drag using a control volume approach is highly dependant on the location of the wake survey plan, and suggest performing measurements at least four chord lengths downstream of the trailing edge. Due to physical constraints, wake measurements were performed at $x/c = 2$ and only the relative change in C_D will be considered.

Spectral analysis of the streamwise velocity was used to identify organized flow structures in the wake and determine their characteristics. For each power spectrum, 2^{18} velocity data points were acquired and split into 64 overlapping (50%) segments each containing 4096 data points. The power spectral density (PSD) of individual segments were computed and averaged. All wake measurements were acquired at a sampling rate $f_s = 5 \text{ kHz}$.

RESULTS

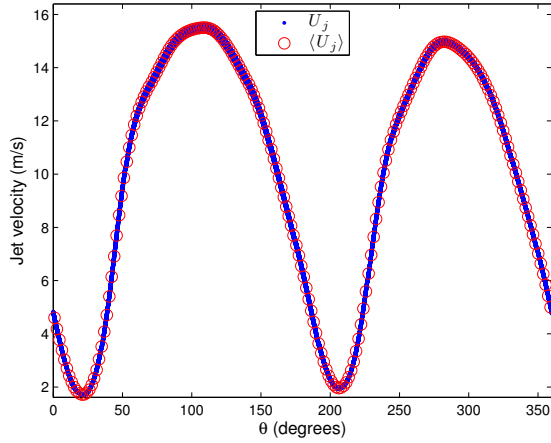
Synthetic jet characterization

The frequency response of the centreline (half-width of the slot) jet velocity was measured at a spanwise location corresponding to the centre of one of the actuators. The frequency was varied from 200 to 1200 Hz in 50 Hz intervals and six input amplitudes were considered (50, 100, 150, 200, 250 and 275 V_{p-p}). Due to the maximum current output of the voltage amplifier (250 mA), the actuators could not be driven at amplitudes greater than 275 V_{p-p} for frequencies above $\sim 1000 \text{ Hz}$.

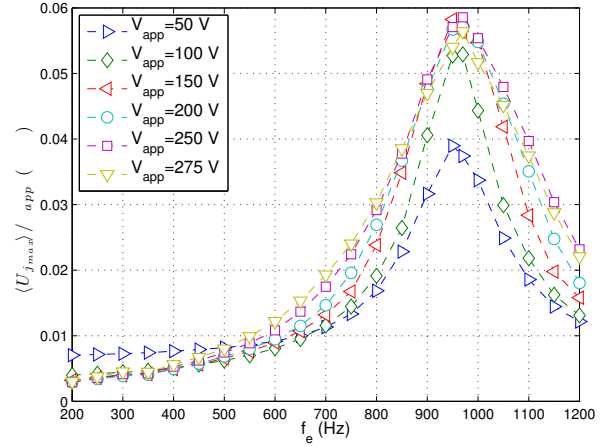
An typical jet velocity profile for an applied voltage $V_{app} = 275 \text{ V}_{p-p}$ and excitation frequency $f_e = 970 \text{ Hz}$ is shown in Figure 4a. The jet velocity is plotted against the phase angle θ , which is measured relative to the driving signal supplied by the function generator. The phase averaged cycle, $\langle U_j \rangle$, was computed from 4848 individual cycles, which are shown plotted together over one cycle (blue markers). The first peak in the velocity profile represents the expulsion phase, and the second represents the ingestion phase. Since a hot-wire probe cannot determine velocity direction, the velocity during the ingestion phase is also positive and reaches a maximum value close to that of the expulsion phase, $\langle U_{j_{max}} \rangle = 15.5 \text{ m/s}$.

The magnitude portion of the maximum exit-plane jet velocity frequency response is shown in Figure 4b. The phase-averaged maximum jet velocity $\langle U_{j_{max}} \rangle$ is converged to within 0.1% at the 95% confidence interval in all cases. Detailed measurements from 950 to 1000 Hz in 10 Hz intervals revealed a peak at 970 Hz for each forcing amplitude. This value can be compared with the Helmholtz frequency of the cavity, given by

$$f_H = \frac{1}{2\pi} \sqrt{\frac{a_c^2 A}{V_c L_{\text{eff}}}} \quad (4)$$



(a) U_j for $V_{app} = 275 V_{p-p}$ and $f_e = 970$ Hz.



(b) Magnitude response of $\langle U_{jmax} \rangle$ for $V_{app} = 50 - 275 V_{p-p}$.

Figure 4: SJA velocity characteristics at the jet exit plane.

where a_c is the isentropic speed of sound in the cavity, A is the slot cross-sectional area, V_c is the cavity volume and L_{eff} is the effective neck length. Equation (4) gives $f_H = 883$ Hz. This value is within 10% of the experimentally determined resonant frequency and indicates that the peak at $f_R = 970 \pm 10$ Hz is due to Helmholtz resonance of the cavity. From the lumped-element model of Gallas *et al.* (2003), a synthetic jet actuator can be modelled as a coupled electromechanical-acoustic system. This model results in a 4th-order system in Fourier space with two resonant frequencies. When the ratio of the acoustic compliance of the diaphragm, C_{aD} , to the acoustic compliance of the cavity, C_{aC} , tends to zero, the SJA behaves as a 2nd-order system with natural frequency $\omega_n = 2\pi f_H$. For the SJA used in this study, $C_{aD}/C_{aC} = 0.05$, therefore a strong resonant peak close to f_H is expected. If the frequency response were extended to higher frequencies, a second peak with much lower magnitude would be expected near the piezoelectric diaphragm natural frequency. Figure 4b also demonstrates that at $f_e = f_R$, for input voltages above 100 V, the SJA behaves relatively linearly since the frequency response is in-

dependent of the voltage amplitude. Tian *et al.* (2007) also found that for low excitation voltages ($V_{app} \leq 50$ V), their SJA behaved nonlinearly.

The velocity profile at the jet exit-plane was used to compute the momentum coefficient C_μ . Figure 5 shows the variation of C_μ with excitation frequency over the range of input voltages considered. The resonant peak offers the largest values of C_μ and thus for this study the SJA was operated at $f_e = 970$ Hz. This corresponds to a dimensionless frequency $F^+ = 48$.

Drag reduction using synthetic jet actuation

Uncontrolled case. The velocity profile of the uncontrolled wake at $\alpha = 10^\circ$ was measured two chord lengths downstream of the airfoils trailing edge ($x/c = 2$). As shown in Figure 6a, the wake extends from approximately $y/c = -0.25$ to 0.7, giving an uncontrolled wake width of $0.95c$. The minimum velocity $(U/U_o)_{min} = 0.82$ occurs at $y/c = 0.25$.

Velocity measurements were taken at several y/c locations to determine the frequency content of the wake. Three points were considered: $(U/U_o)_{min}$, $U/U_o = 0.98$ above $y = 0$, and $U/U_o = 0.98$ below $y = 0$. No evidence of coherent structures in the wake was seen in the power spectrum corresponding to $(U/U_o)_{min}$, however both $U/U_o = 0.98$ locations showed distinct spectral peaks at the same frequency. All PSD subsequent measurements were taken at $U/U_o = 0.98$ above $y = 0$.

Figure 6b shows the PSD of the streamwise velocity (u) measured at $x/c = 2$. The power spectra is normalized by the variance of u . A distinct peak at $f_{wake} = 11$ Hz is seen. The normalized frequency can be described by a Strouhal number, $St_L = fL/U_\infty$, where L is the vertical length of the airfoil projected on a cross-stream plane. The peak at 11 Hz corresponds to $St_L = 0.19$, which agrees well with $St_L = 0.22$ as reported by Yarusevych *et al.* (2006) for a NACA 0025 airfoil at $\alpha = 10^\circ$. The proximity of $St_L = 0.19$ to $St_L = 0.2$, the characteristic shedding frequency of a circular cylinder, suggests that the peak at f_{wake} corresponds to vortex shedding similar to that of a bluff body.

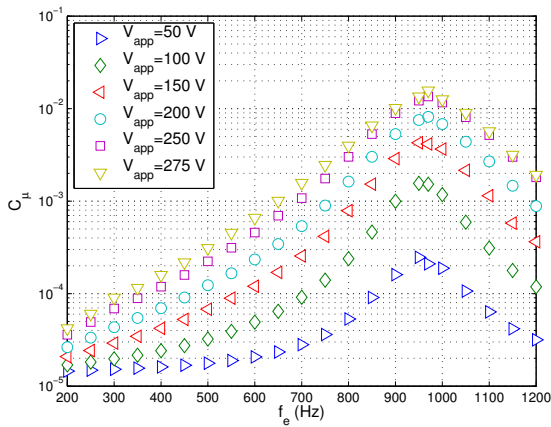
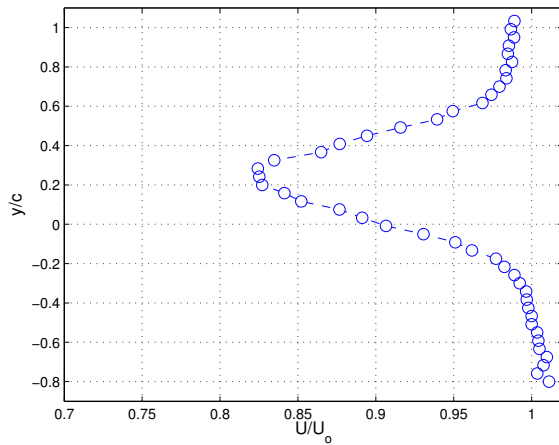
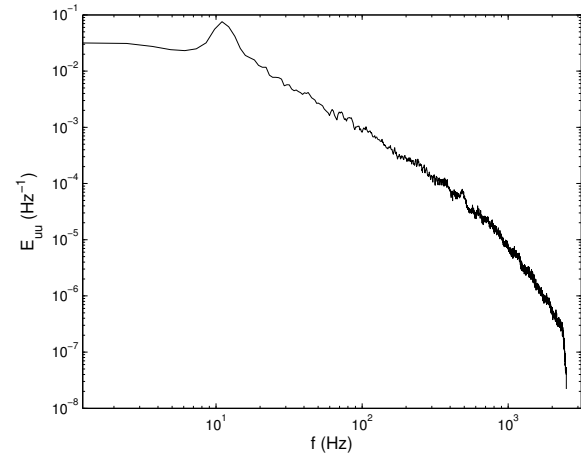


Figure 5: Momentum coefficient variation with excitation frequency and voltage.



(a) Wake profile.



(b) Power spectral density of streamwise velocity at $U/U_o = 0.98$.

Figure 6: Wake characteristics at $x/c = 2$ and $\alpha = 10^\circ$ with no control ($C_\mu = 0$).

Constant excitation frequency forcing.

The synthetic jet actuator was driven at $f_e = 970$ Hz and the voltage amplitude was varied from 50 to 400 V_{p-p} to achieve different forcing levels. Two voltage amplifiers were used to overcome the initial limitation of operating at voltages above 275 V_{p-p} . The momentum coefficient was varied from $C_\mu = 2.10 \times 10^{-4}$ at $V_{app} = 50$ V to $C_\mu = 2.74 \times 10^{-2}$ at $V_{app} = 400$ V.

Figure 7 shows a comparison of the uncontrolled wake profile to the controlled cases with $C_\mu = 0.0157$ and $C_\mu = 0.0274$. As the momentum coefficient is increased, the minimum wake velocity increases slightly to $(U/U_o)_{min} \approx 0.85$ and the wake centre is shifted towards $y = 0$. This suggests that the flow has been at least partially reattached. Furthermore, increasing C_μ to 0.0274 causes the wake width to decrease to $\sim 0.78c$ (an 18% decrease from the uncontrolled case). The upper boundary of the wake remains constant at $y/c \approx 0.3$ while the lower wake boundary shifts in the $-y$ direction. Similar behaviour was seen at $\alpha = 5^\circ$ by Goodfellow *et al.* (2012); increasing C_μ resulted in increasing $(U/U_o)_{min}$, decreasing wake width and shifting of the wake

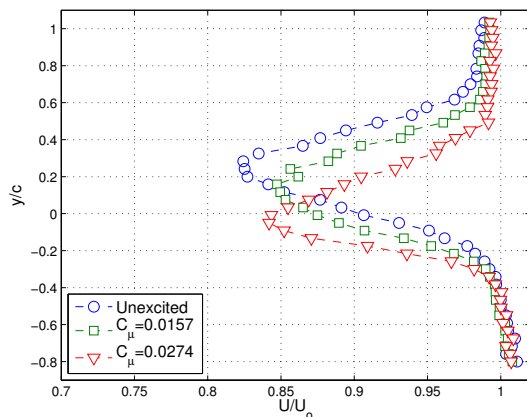


Figure 7: Wake profiles at $x/c = 2$ for $\alpha = 10^\circ$ and forcing at $f_e = 970$ Hz.

centre towards $y = 0$.

The PSD of the streamwise velocity at each forcing amplitude is shown in Figure 8. For clarity, the amplitude of each successive power spectrum is increased by an order of magnitude. As C_μ is increased, the spectral peak at $f_{wake} = 11$ Hz associated with vortex shedding in the wake is flattened until it is no longer apparent. This trend was also observed by Goodfellow *et al.* (2012) at $\alpha = 5^\circ$. When the flow becomes reattached, it is expected that the dominant coherent structure in the wake will have decreased length scale and correspond to a weaker spectral peak. Since the transverse velocity component (v) is more sensitive to these weak fluctuations, the PSD of v may provide insight into the wake characteristics of the attached flow. Future work will include crosswire measurements in the wake in order to compute E_{vv} .

The variation in the drag coefficient, C_D , relative to the baseline drag coefficient, C_{D_o} , with C_μ is shown in Figure 9. The results of this investigation at $\alpha = 10^\circ$ and $Re_c = 10^5$ are shown along with the results at $\alpha = 5^\circ$ by Goodfellow *et al.* (2012) using the same airfoil/test facility and measured at $x/c = 2$. The results show that in each case, the drag coefficient is relatively constant until a threshold value of C_μ is reached, after which a substantial drop occurs. At 5° , a much lower value of C_μ is required to effect this decrease in C_D . Furthermore, the change in C_D is much more drastic for $\alpha = 5^\circ$. In the present experiments, C_D begins to decrease appreciably at $C_\mu = 0.0157$ and reaches a value of $0.78C_{D_o}$ at the highest achievable momentum coefficient, $C_\mu = 0.0274$. If the measurements at $\alpha = 10^\circ$ were extended to higher values of C_μ , it is possible that C_D/C_{D_o} would follow the same trend as $\alpha = 5^\circ$. That is, the initial increase in C_μ above the threshold level produces a significant decrease in C_D , with the positive effect saturating at higher values of C_μ .

CONCLUSION

Synthetic jet actuation was used to promote flow reattachment and improve aerodynamic performance on a NACA 0025 airfoil experiencing laminar boundary layer separation at $Re_c = 10^5$ and $\alpha = 10^\circ$. Characterization of

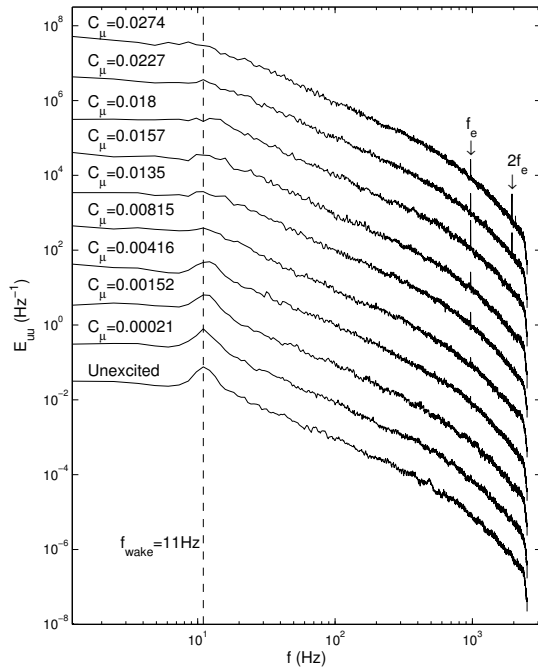


Figure 8: Power spectral density of the steamwise velocity at $x/c = 2$ for $\alpha = 10^\circ$ and forcing at $f_e = 970$ Hz.

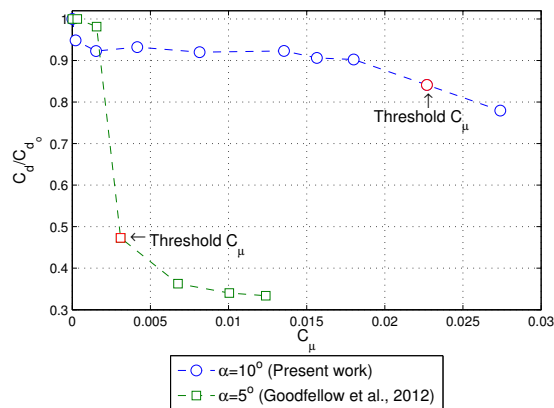


Figure 9: Drag coefficient variation with C_μ at $Re_c = 10^5$ for constant excitation frequency.

the SJA in quiescent conditions revealed a resonant peak at 970 ± 10 Hz where the jet velocity was maximized.

In the uncontrolled case, the airfoil wake showed a dominant vortex shedding frequency $f_{\text{wake}} = 11$ Hz ($F^+ = 0.54$). Actuation at an excitation frequency $f_e = 970$ Hz ($F^+ = 48$) and momentum coefficient $C_\mu = 0.0247$ was

able to eliminate the large-scale shedding associated with f_{wake} and decrease the uncontrolled wake width by 18%. This led to a 22% decrease in the drag coefficient.

The results from this work and previous experiments at $\alpha = 5^\circ$ by Goodfellow *et al.* (2012) suggest that to achieve appreciable drag reduction, a threshold value of C_μ is required when the forcing is applied at an excitation frequency much larger than the dominant wake frequency ($f_e \gg f_{\text{wake}}$). At $\alpha = 10^\circ$, the threshold value of C_μ is ~ 10 times larger than that at $\alpha = 5^\circ$. Future work will involve performing the same measurements at other angles of attack between $0 - 10^\circ$ in order to further investigate the influence of C_μ on flow reattachment and drag reduction.

ACKNOWLEDGEMENTS

The authors gratefully acknowledge support from the Natural Sciences and Engineering Research Council of Canada.

REFERENCES

- Amitay, Micheal, Smith, Douglas R., Kibens, Valdis, Parekh, David E. & Glezer, Ari 2001 Aerodynamic Flow Control over an Unconventional Airfoil Using Synthetic Jet Actuators. *AIAA Journal* **39** (3).
- Gallas, Quentin, Holman, Ryan, Nishida, Toshikazu, Carroll, Bruce, Sheplak, Mark & Cattafesta, Louis 2003 Lumped Element Modeling of Piezoelectric-Driven Synthetic Jet Actuators. *AIAA Journal* **41** (2), 240–247.
- Goodfellow, Sebastian D., Yarusevych, Serhiy & Sullivan, Pierre E. 2012 Momentum coefficient as a parameter for aerodynamic flow control with synthetic jets. *AIAA Journal* **51**, 623–631.
- Greenblatt, David & Wygnanski, Israel J. 2000 The control of flow separation by periodic excitation. *Progress in Aerospace Sciences* **36** (7), 487–545.
- Lissaman, P. B. S. 1983 Low-Reynolds-Number Airfoils. *Annual Review of Fluid Mechanics* **15**, 223–239.
- Neatby, H. C. & Yarusevych, S. 2012 Towards Reliable Experimental Drag Measurements on an Airfoil at Low Reynolds Number. 42nd AIAA Fluid Dynamics Conference.
- Reynolds, W. C. & Hussain, A. K. M. F. 1972 The mechanics of an organized wave in turbulent shear flow. part 3. theoretical models and comparisons with experiments. *Journal of Fluid Mechanics* **54** (02), 263–288.
- Smith, Barton L. & Glezer, Ari 1998 The formation and evolution of synthetic jets. *Physics of fluids* **10**, 2281.
- Tian, Ye, Cattafesta, Louis & Mittal, Rajat 2007 Adaptive control of separated flow. *AIAA paper* pp. 1–11.
- Van Dam, C. P. 1999 Recent experience with different methods of drag prediction. *Progress in Aerospace Sciences* **35** (8), 751–798.
- Yarusevych, Serhiy, Sullivan, Pierre E. & Kawall, John G. 2006 Coherent structures in an airfoil boundary layer and wake at low Reynolds numbers. *Physics of Fluids* **18** (4), 044101.